Biological effects, including oxidative stress and genotoxic damage, of polystyrene nanoparticles in different human hematopoietic cell lines

Laura Rubio[1], Irene Barguilla[2], Josefa Domenech[2], Ricard Marcos[2,3,*], Alba Hernández[2,3,*]

[1]Nanobiology Laboratory, Department of Natural and Exact Sciences, Pontificia Universidad Católica Madre y Maestra, PUCMM, Santiago de los Caballeros, Dominican Republic.

[2]Department of Genetics and Microbiology, Faculty of Biosciences, Universitat Autònoma de Barcelona, Cerdanyola del Vallès (Barcelona), Spain.

[3]Consortium for Biomedical Research in Epidemiology and Public Health (CIBERESP), Carlos III Institute of Health, Madrid, Spain.

[*]Corresponding authors at: Grup de Mutagènesi, Departament de Genètica i de Microbiologia, Facultat de Biociències, Universitat Autònoma de Barcelona, Campus de Bellaterra, 08193 Cerdanyola del Vallès (Barcelona), Spain. Phone: +34 93 581 20 52; Fax: +34 93 581 23 87.

E-mail address: ricard.marcos@uab.es

alba.hernandez@uab.es

Running Title: Different effects of nanopolystyrene according to the cell line

Abstract

In recent years the terms "micro-/nanoplastics" (MNPLs) have caught special attention due to the increasing levels by which humans are exposed. Among MNPLs, polystyrene nanoparticles (PSNPs) are one of the most represented MNPLs in the environment. These tiny particles may enter into the human body, translocate through human barriers, interacting with blood and lymphatic immune cells, and reaching secondary organs. By using three different human leukocytic cell lines: Raji-B (B-lymphocytes), TK6 (lymphoblasts) and THP-1 (monocytes), we pursued to determine the effects of these PSNPs on the immune cell population. With this aim, the three cell lines were exposed to spherical PSNPs of about 50 nm of diameter and cytotoxicity, cellular uptake, reactive oxygen species (ROS) production, and genotoxicity were assessed at different time-points. Results show differences in all the measured endpoints, among the selected cell lines. Thus, whilst the monocytic THP-1 cells showed the highest particle internalization, no adverse effects were observed in such cells. On the other side, although Raji-B and TK6 showed lesser PSNPs uptake, mild toxicity, ROS production and genotoxicity were detected. These results highlight the importance of the cell line selection when the biological effects of PSNPs are evaluated.

Keywords: Polystyrene nanoparticles, ROS, genotoxicity, THP-1, Raji-B, TK6

1. Introduction

Micro-/nanoplastics (MNPLs) contamination has become a global concern since the presence of these ubiquitous and tiny particles (< 5,000 μm) is rapidly increasing in all the environments and ecosystems. A recent study estimates that the ocean is contaminated by 8.3 million MNPLs per cubic meter of water, a million times more than previously estimated (Brandon et al., 2020). The origin of this contamination mainly (60 - 80%) comes from the degradation of the accumulated plastic waste giving rise to the so-called secondary MNPLs (Andrady, 2003; Hesler et al., 2019). On the other side, the contamination of primary MNPLs (the intentionally “micron and nano-size” synthesized particles for industrial applications), comes mainly from cosmetics and personal care products (Napper et al., 2015). Regardless of the origin of these particles, its direct and continuous contact with human beings has arisen many questions about the potential health effects, which are still not completely answered.

Among the plastic polymers, polystyrene (PS) is a highly synthesized and versatile material used in different industrial applications such as food packaging, electronics, automotive sector, containers for transportation, and house appliances, among many others (ChemicalSafetyFacts.org). In biomedicine, PS has also been used in diagnostic components, in tissue culture trays, test tubes, Petri dishes, medical devices, and in form of nanoparticles in pharmacological studies (Loos et al., 2014; Lehner et al., 2019). Besides the suitability of this product for the production of so many consumer products, the low economic cost has perpetuated its industrial growth. Due to the high production on one hand, and its extreme resistance to being degraded, on the other hand, the generated primary and secondary PS-MNPLs are accumulating in all the ecosystems. In this way, they are becoming one of the top three MNPLs found in nature, and a great environmental problem (Tokiwa et al., 2009; Loos et al., 2014; Bouwmeester et al., 2015; Galloway, 2015). Consequently, the internal presence of PS-MNPLs has already been detected in a wide variety of organisms (Wright et al., 2013; Gallo et al., 2018).

Although the scientific studies are growing fast in this area, there is still a general lack of knowledge about the biological effects, in *in vitro* and *in vivo* mammalian models, of MNPLs in general, and PS-MNPLs in particular (Rubio et al., 2019). Nevertheless, the use of PS nanoparticles (PSNPs) in biomedicine, as a model in pharmacological studies, has provided additional information about its related biological effects. Among the different toxicity studies carried out using PS-MNPLs in *in vitro* or *in vivo* mammalian models, controversial results have appeared. Thus, whilst some authors (Fröhlich et al., 2012; Loos et al., 2014; Stock et al., 2019; Hesler et al. 2019; Cortés et al., 2019) showed minor or no adverse effects of PS-MNPLs in their investigations, other studies reported the induction of oxidative stress, genotoxicity, cytotoxicity, necrosis or inflammation (Forte et al., 2016; Schirinzi et al., 2017; Deng et al., 2017; Wu et al., 2019; Lim et al., 2019).

The potential interactions among these particles and cellular structures occur mainly through ingestion and inhalation. In fact, PS-MNPLs have repeatedly proved its capacity to translocate the mucosa tissues (intestinal and airway epithelial barriers) arriving at the blood and lymphatic circulation (Jani, 1990, 1992; Hussain et al., 2001; Wright and Kelly, 2017). This ability allows these particles to interact with different organs and cell types being blood and lymphatic immune cells a direct target. However, the effects that this interaction could provoke in these types of cells are not well known. To fill in this gap, three different and well-known leukocytic cell lines: TK6 lymphoblastic, Raji-B lymphocytes, and THP-1 monocytic cells, have been used in this study in order to identify possible effects of PSNPs exposure regarding cytotoxicity, cellular uptake, reactive oxygen species (ROS) production, and genotoxic damage induction. The use of these cell lines can help us to understand potential effects on blood cells after *in vivo* exposures.

2. Experimental methods

2.1. PSNPs characterization

PSNPs were commercially obtained from Spherotech (Chicago, USA). Two different types of PSNPs in the nanoscale were purchased, differing on its fluorescence. Pristine PSNPs (PSNPs, ref. PP-008-10) with a nominal size ranging from 0.05 to 0.1 µm and fluorescent PSNPs (fPSNPs, ref FP-00552) with size range from 0.04 to 0.09 µm were used, depending on the nature of the experiments. As previously described, dispersions of both types of PSNPs were prepared at 100 µg/mL in distilled water, and in the cell culture medium (RPMI, 10% fetal bovine serum (FBS)), and were further characterized (Cortés et al., 2020). Transmission electron microscopy (TEM) was used to determine the shape and size of particles on a JEOL JEM-1400 instrument (Jeol LTD, Tokyo, Japan). Additionally, dynamic light scattering (DLS) and laser Doppler velocimetry (LDV) methodologies (Malvern Zetasizer Nano ZS zen3600, Malvern, UK) were used to measure the hydrodynamic size and Z-potential parameters, respectively.

2.2. Cell culture

Three different lymphoblastic human cell lines were used for this study: THP-1 (monocytes), TK6 (lymphoblasts), and Raji-B (B-lymphocytes). All they were purchased from Sigma Aldrich (MO, USA). The selection of these immune-related cell lines was based on the fact that they are widely used as a model of human hematopoietic cells. The three cell lines were cultured in suspension in 25 cm^2 culture flasks with RPMI (Biowest, France) supplemented with 10% FBS, 1% glutamine (Biowest, France) and 2.5 µg/mL Plasmocin™ (InvivoGen, CA, USA). Cells were maintained in a range from 5 x 10^5 cells/mL to 1 x 10^6 cells/mL in a humidified atmosphere of 5% CO_2 and 95% air at 37 ºC.

2.3. Cell viability

The three cell lines were seeded, independently, on 96 well plates at a density of 5 x 10^5 cells/mL, and exposed to a range of concentrations from 0 µg/mL up to 200 µg/mL of PSNPs during 24 and 48 h to perform the toxicity assessment. After the exposure, toxicity was measured by using the Trypan Blue (Sigma Aldrich, MO, USA) exclusion assay. Cells were thoroughly mixed in a 1:1 ratio with 0.4% Trypan Blue; then, 10 µL of the stained sample was charged into the Neubauer chamber for cell counting. Only dead cells will be blue-stained due to membrane permeability. Cell viability was calculated as follows:

% Viability = [1.00 – (Number of dead cells ÷ Number of total cells)] × 100

The final viability values were determined by averaging three independent viability experiments. Each experiment was performed using two replicates per each concentration.

2.4. Cell internalization

The ability of cells to internalize fPSNPs was assessed by flow cytometry. Cell suspensions of the three different cell lines, at a density of 5 x 10^5 cells/mL, were seeded in 96 well plates, and treated with the following concentrations of fPSNPs; 1, 5, 10, 25 and 50 µg/mL, for exposures lasting for 24 and 48 h. After the treatments, cells were collected, centrifuged and the pellet resuspended to 1 x 10^6 cells/mL in 1X PBS. The intracellular fluorescence was measured by using FACS Canto with excitation/emission spectra of 488/585 nm, respectively. For each concentration, a total of 20,000 cells were scored. Data were evaluated using the BD FACSDiva software. Three independent experiments were carried out using duplicates for each concentration.

2.5. Reactive oxygen species quantification

The intracellular generation of ROS was measured by flow cytometry using the dichlorodihydrofluorescein diacetate assay (DCFH-DA, Sigma Aldrich). Cellular

159 suspensions at a density of 5 x 10^5 cells/mL of the three different cell lines were
160 seeded independently in 96 well plates and treated with the following concentrations of
161 PSNPs; 5, 10, 25 and 50 µg/mL, for exposure lasting for 3 and 24 h. Subsequently,
162 cells were centrifuged and incubated in the presence of 5 µM DCFH-DA in serum-free
163 RPMI medium for 30 min at 37 °C. After DCFH-DA exposure, cells were collected,
164 centrifuged and the pellet resuspended to 1 x 10^6 cells/mL in 1X PBS. Cells were
165 immediately analyzed by using a FACS Canto. A number of 20,000 cells were scored
166 and evaluated using the BD FACSDiva software. A minimum of three independent
167 experiments was carried out.
168
169 *2.6. The comet assay*
170 Both, the general genotoxic, and the specific oxidative DNA damage (ODD), of
171 PSNPs at 3, 24 and 48 h of exposure, were evaluated by the alkaline comet assay with
172 and without the use of formamidopyrimidine DNA glycosylase (FPG) enzyme, as
173 previously described (Annangi et al., 2015). Briefly, after the exposure, cell
174 suspensions were collected and centrifuged at 130 g for 8 min. The pellet was washed
175 and resuspended at 1x10^6 cells/mL in cold 1X PBS at 4 °C. Cells were mixed (1:10)
176 with 0.75% low melting point agarose at 37 °C and dropped onto GelBond® films
177 (GBFs) (Life Sciences, Lithuania). Cells on GBFs were lysed overnight submerged in
178 cold lysis buffer at 4 °C. Later on, GBFs were gently washed twice (5 and 50 min) in
179 enzyme buffer at 4 °C followed by an extra 30 min incubation, without (for general
180 genotoxicity quantification) or with (for ODD quantification) the FPG enzyme at a
181 1:25,000 dilution at 37 °C. FPG enzyme was produced in our laboratory, and a
182 concentration of 0.0089 µg/µL of enzyme extract was used in each treatment. After
183 that, GBFs were rinsed with electrophoresis buffer for 5 min and left in new
184 electrophoresis buffer for 25 min, to allow for DNA unwinding and expression of alkali
185 labile sites. Electrophoresis was carried out for 20 min at 20 V and 300 mA at 4 °C.
186 Then, the GBFs were rinsed twice in cold 1X PBS for 5 and 10 min, fixed in absolute

ethanol (VWR, PA, USA) for 2 h, air-dried overnight at room temperature and stained for 20 min with 1:10,000 SYBR Gold (Life Technologies, NY, USA) in TE buffer. Finally, gels were visualized for comets using an epifluorescent microscope (Olympus BX50) at 20X magnification. The quantification of DNA damage in cells was done measuring the percentage of DNA in the tail by using the Komet 5.5 Image analysis system (Kinetic Imaging Ltd, Liverpool, UK). One hundred randomly selected comet images were analyzed per sample. Two different samples were analyzed for each condition in each one of the three experiments performed. Methanesulfonate (MMS) (Sigma-Aldrich, Germany) at 200 µM was used for 30 minutes as a positive control for both, general genotoxic and oxidative genotoxic damage.

2.7. Statistical analysis

Statistical analyses were performed using GraphPad Prism 5 software. Three experiments were carried out by each one of the evaluated targets. Data were analyzed using one-way ANOVA with Dunnett's post-test. Statistical significance was defined as *P ≤ 0.05, **$P \leq 0.01$, ***$P \leq 0.001$.

3. Results

3.1. PSNPs characterization

Morphology and size of PSNPs and fPSNPs were determined using TEM (Figure 1). As indicated by the manufacturer, pristine spherical particles of about 50 nm in diameter were observed in both PSNPs and fPSNPs. When the hydrodynamic size was analyzed in culture medium (RPMI) and in distilled water, by using DLS, higher dimensions compared to TEM analysis were achieved due to particle aggregation. Thus, as observed in Table 1, differences in hydrodynamic sizes also appeared regarding the dispersant with higher aggregation corresponding to the culture medium. Consistently, Z-potential values showed more stable solutions of PSNPs when diluted in distilled water.

3.2. Cell viability

Cell viability curves were carried out to determine the cytotoxicity related to PSNPs exposure on the three selected cell-lines. For this purpose, THP-1, TK6, and Raji-B cells were exposed for 24 and 48 h to a range of concentrations up to 200 µg/mL. As shown in Figure 2 no significant cytotoxicity effects were observed in any of the cell lines up to the concentration of 100 µg/mL. Only mild effects were observed at the very high tested concentration (200 µg/mL), compromising the viability of TK6 and Raji-B cell lines to 80% after exposures lasting for 24 h (Figure 2A), and slightly higher effects at 48 h (Figure 2B). In this regards the monocytic THP-1 cell line seems to be the more resistant cell line after the highest exposure. Since our aim was to work with non-toxic and more relevant doses, lower concentrations were used for the rest of the assays.

3.3. PSNPs cellular internalization

The cellular uptake of fPSNPs was evaluated, by using flow cytometry, in the three selected cell lines after exposures lasting for 24 and 48 h to a range of concentrations (1, 5, 10, 25 and 50 µg/mL). Very high internalization rates were observed in the three

cell lines at both exposure times. As shown in Figure 3 at the highest concentration of 50 µg/mL almost 100% of the cells contained fluorescent particles in the three cell lines. At lower concentrations, differences in the levels of uptake among cell lines were observed, the monocytic THP-1 cells showing the highest ability to internalize particles, whereas the Raji-B cells were the less prone to internalize fPSNPs.

3.4. Intracellular ROS induction

Oxidative stress is one of the highlighted mechanisms by which MNPLs could be causing cellular damage (Wright and Kelly, 2017). In our experiments, intracellular ROS were quantified after THP-1, TK6 and Raji-B cells were exposed to PSNPs (5, 10, 25 and 50 µg/mL) for 3 and 24 h. Figure 4A shows a significant peak of ROS production at the highest concentration after 3 h of treatment in TK6 cells, and also significant values in Raji-B cells. Lower, but substantial ROS production was quantified after 24 h of treatment in all the tested concentrations in TK6 cells (Figure 4B). Interestingly, THP-1 cells did not produce significant increases of ROS in any of the concentrations evaluated, or in any of the exposure times used.

3.5. Induction of genotoxic damage and ODD by PSNPs exposure

The comet assay, an OCDE approved protocol for genotoxicity assessment, complemented with the use of the FPG enzyme for ODD quantification was applied in this study. Three different time points, 3, 24 and 48 h were assessed, using the three selected cell lines. Regarding Raji-B cells, although no effects were observed at 3 h of exposure to PSNPs (Figure 5A), significant increases in the levels of general genotoxic damage were quantified at 24 and 48 h of exposures to 25 and 50 µg/mL (Figures 5B, 5C). As shown in Figure 5B, ODD was only detected after exposures lasting for 24 h, and at the highest tested concentration (50 µg/mL). On the contrary, the percentage of DNA in the tail of TK6 cells exposed to PSNPs was not significantly higher than the detected in non-exposed cells, at any of the duration treatments or concentrations

tested (Figure 6). However, when the assay was complemented with FPG, ODD was detected in all the concentrations at exposure lasting for 24 h (Figure 6B), and at the concentrations of 10 and 25 µg/mL after 48 h of treatment (Figure 6C). Finally, Figure 7 shows the lack of genotoxicity or ODD related effects observed in THP-1 cells exposed to PSNPs. These negative effects were observed independently of the exposure and time points evaluated. As an effective positive control, MMS produced both general genotoxicity and ODD effects in all the conducted experiments.

4. Discussion

The objectives of our study were diverse. The first aim was to increase the database of studies using mammalian/human cells, and the detection of effects related to potential health effects of MNPLs exposures. The second was to test the susceptibility of hematopoietic cells, as potential human targets, to present adverse effects after MNPLs exposures once MNPLs cross the biological barriers. Finally, to detect different sensitivities to MNPLs between the different hematopoietic cells used was another aim. Our results clearly show that hematopoietic cells were able to internalize PSNPs and produce both intracellular ROS and genotoxicity, although important differences between cell lines were observed.

It is remarkable the ability of PSNPs to be incorporated into the hematopoietic cells selected in our study. In fact, our results confirm the great particle internalization previously observed in other human cells, such as the intestinal Caco-2 cells. In such a case, the cellular uptake was modulated by both the exposure levels and exposure times (Cortés et al., 2020). The uptake of PS at the microsize level (1-10 µm) was also evaluated in Caco-2 cells, both undifferentiated and differentiated, showing the highest uptake when PS sized 4 µm were used (Stock et al., 2019). Furthermore, cell uptake of PSNPs was also demonstrated in human pulmonary cells BEAS-2B (Lim et al., 2019). Unfortunately, these last two studies did not use flow cytometry to quantify the uptake, alternatively, they used semi-quantitative approaches such as fluorescent and confocal microscopy. Although testing the effects of polyethylene terephthalate (PET) nanoplastics, other authors have also used flow cytometry to quantify its uptake (Magrì et al., 2018). The authors obtained the kinetics profile over time of the PET uptake, by monitoring the mean fluorescence values from flow cytometry distributions of ≥100,000 Caco-2 cells, showing that cell fluorescence intensity linearly increased, but without reaching the saturation. In our case, we evaluated the percentage of cells that uptake the fPSNPs showing that at the highest doses the 100% of the cells incorporated the fluorescent signal, as indicative of fPSNPs uptake. According to all these data, it seems

295 that flow cytometry can be a useful approach to test, not only the percentage of cells
296 uptaking PSNPs but also to determine how many fPSNPs have been incorporated into
297 each cell, according to the intensity of the fluorescent signal (Cortés et al., 2020). It is
298 also remarkable the finding that cellular uptake is modulated by the different types of
299 hematopoietic cells used. These differences are observable at low doses; thus, at 1
300 µg/mL and exposures lasting for 24 h, only THP-1 cells were able to incorporate
301 significant amounts of fPSNPs. At the dose of 5 µg/mL, the differences between cells
302 are much more appreciable with the following ranking THP-1 > TK6 > Raji-B. The high
303 ability of THP-1 to incorporate PSNPs can be associated with the uptake efficacy of
304 phagocytic cells such is the case of THP1 cells. In fact, THP-1 cells differentiated into
305 M0, M1 and M2 macrophages were used to determine the cell uptake of PS at the
306 microsized range observing an important uptake but only for PS sized 4 µm. These
307 studies were carried out using fluorescent microscopy (Stock et al., 2019).

308 Potential interactions between PSNPs and some plasma components have been
309 recently reported (Gopinath et al., 2019). Authors showed that plasma proteins can
310 display strong affinity with PSNPs producing a surrounding corona, inducing a protein-
311 induced coalescence. This process could modify the potential biological effects of
312 PSNPs, including its uptake. As above indicated, in our case that mechanism does not
313 seems to affect the uptake ability, that it is mainly modulated by the cell type.

314 Despite the important cellular uptake, results indicate that no effects on the cell
315 viability are induced by PSNPs. The mild effects detected at very high concentrations
316 are not relevant from the environmental point of view. This lack of toxicity was also
317 reported for other human cells lines such us the undifferentiated intestinal Caco-2 cells
318 (Inkielewicz-Stepniak et al., 2018; Magrì et al., 2018; Cortés et al., 2020). Similarly, no
319 toxic effects were obtained testing the brain (T98G) and the epithelial (HeLa) human
320 cell lines (Schirinzi et al., 2017). No studies have been found in the literature
321 determining differences between cell types exposed to PSNPs evaluating the role of
322 cell type in front of PSNPs exposures. Nevertheless, it is well known that different cell

types respond differently to xenobiotics (Xia et al., 2008; Gies and Zou, 2017). By comparing the sensitivity of six cell lines towards the toxic effects of graphene oxide, a great variability between cell lines was observed, showing the suspension cells a greater response to the GO treatment compared to the adherent cell lines (Gies and Zou, 2017). These differences cannot be observed in our study because the three selected cell lines grows in suspension. Interestingly, in our study no associations between cell uptake and toxicity are observed, supporting the lack of toxicity of pristine PSNPS. It should be remarked that this lack of toxicity of pristine PSNPs could not be directly extrapolated to environmental PSNPs resulting from higher sized plastics. Environmental PSNPs, resulting from the degradation of macroplastics carry different types of additives (such as phthalates) used as plasticizers during the process of production that can be toxic (Ma et al., 2019). Furthermore, during their long life in the environments, they can adsorb different types of environmental pollutants such as organic compounds and heavy metals (Yu et al., 2019; Davranche et al., 2019).

To detect environmental factors that can act as risk modulators in disease, different biomarkers are proposed including the overproduction of ROS, which could play a role in disease through oxidative stress (Ghezzi, 2020). This biomarker is one of the parameters usually evaluated when testing the effects of nanomaterials, including nanoplastics. Although many *in vivo* studies using aquatic organisms have reported ROS induction, the *in vitro* studies are inconclusive. Thus, when larvae of zebrafish exposed to PSNPs were treated with DCFDA, as a green fluorescent ROS reporter, fluorescence was detected through the whole body, especially in the head region (Sökmen et al., 2019). In a similar way, when *Daphnia pulex* was exposed to PSNPs, an overproduction of ROS was observed increasing the expression of the MAPK-HIF-1/NFkB pathway, resulting in inhibited growth, development, and reproduction (Liu et al., 2020). In *in vitro* studies, ROS induction was evaluated for both polystyrene (10 µm) and polyethylene (3-16 µm) exposures in cerebral (T98G) and epithelial (HeLa) human cells. The study used DHE as a fluorescent marker and positive effects were

only obtained when the highest concentrations of PS were used (Schirinzi et al., 2017). Additionally, positive effects were reported in the human fibroblast Hs27 cell line by using a total ROS assay kit. Nevertheless, the effects were only observed after short exposure times (less than 30 min) (Poma et al., 2019). On the other side, we have recently reported negative ROS induction in human intestinal Caco-2 cells in exposures to PSNPs lasting for 24 h (Cortés et al., 2020). These negative findings would agree with the results reported in this study for THP-1 cells where no effects in ROS production were observed. Mild positive effects were observed in Raji-B cells only when they were exposed to the highest concentration (50 µg/mL) after 3 h of treatment. On the other side, PSNPs were able to induce significant increases of intracellular ROS levels in TK6 cells, for both time and exposure used. This would reinforce the interest of using different cell lines to evaluate the effects induced by PSNPs since such effects can be strongly modulated by the characteristics of the used cell line.

Another useful biomarker to detect potential risk factors associated with environmental factors is genotoxicity, playing a major role in the initiation and progression of different health problems. In fact, it is well known that DNA damage can lead to different relevant consequences as mutation, carcinogenesis, aging, and cell death, among others (Barabadi et al., 2019). In spite of the relevance of this biomarker, very few studies have evaluated the potential genotoxic effects of PSMNPLs and most of them have been conducted in aquatic organisms. In those studies, hemocytes of mussels and clams have been the cell target, and the comet assays the tool to detect the induction of DNA damage. Thus, polystyrene and polyethylene (<100 µm) were able to induce DNA damage in mussel hemocytes (Avio et al., 2015). In a similar way microparticles of polystyrene (20 µm) induced strand breaks in the hemocytes of clams (Ribeiro et al., 2017). Another study also evaluating the exposure of PSNPs (110 nm) in hemocytes of mussels produced significant levels in the percentage of DNA quantified in the tail of the comets (Brandts et al., 2018). It should be remembered that hemocytes are the cells in mollusk playing a similar role than blood white cells in

379 mammalian. Therefore, in some sense, these cells are physiologically similar to those
380 used in our study. Two further recent studies reported data on the genotoxicity of
381 PSNPs in human cells. Although positive effects in the induction of micronuclei were
382 reported in human lymphocytes exposed *in vitro*, no experimental confirmatory data
383 was presented in the paper (Mishra et al., 2019). Another study using human fibroblast
384 Hs27 cells, and the same biomarker of genotoxicity (micronucleus test) reported
385 positive increases in the different parameters evaluated, showing an increased
386 formation of micronuclei and nuclear buds (Poma et al., 2019).

387 Regarding our data, the first notable results are the lack of relationship between
388 uptake and effects. Thus, similarly to what was observed in the induction of ROS, the
389 monocyte THP1 cells did not show any genotoxic effect when exposed to PSNPs. This
390 resistance to show adverse effects associated with PSNPs exposure could be related
391 to its role as macrophages. Higher resistance of THP1 cells compared to other cell
392 lines was detected when exposed to titanium dioxide and silver nanoparticles (Lankoff
393 et al., 2012). Interestingly, both TK6 and Raji-B cells were able to show increased
394 levels of genotoxic damage when exposed to PSNPs, although by using different
395 mechanisms. It is interesting to point out the high versatility of the comet assay to
396 detect different types of damage on the DNA target. Thus, the incubation of treated
397 cells with DNA repair enzymes such as formamidopyrimidine DNA glycosylase (FPG),
398 which detects 8-oxoguanine and other purine oxidation adducts, permits that
399 oxidatively damaged DNA bases converts into DNA breaks. In this way, the assay can
400 quantify both, direct DNA breaks (genotoxic damage) and oxidative DNA damage
401 (ODD) (Cortés et al., 2019). In our study by using FPG, ODD was detected in the TK6
402 cell line exposed to PSNPs for 24 h and 48 h. This would confirm the reiterated high
403 levels of ROS previously observed only in this cell line. Alternatively, although positive
404 induction of DNA breaks was observed in Raji-B cells this damage was observed in the
405 absence of FPG. This would indicate two different modes of action of PSNPs
406 according to the cell type. The high levels of induced ROS and ODD in TK6 cells agree

with the results reported by other authors with this cell line. Thus, using five different cell lines exposed to cobalt-ferrite nanoparticles, TK6 cells were those reporting higher levels of ROS (Horev-Azaria et al., 2013). The genotoxic effects observed in Raji-B cells in absence of FPG would indicate some type of direct effect of PSNPs on DNA. No data has been found showing special characteristics of this cell line explaining its different behavior regarding the observed genotoxic effects. Nevertheless, it must be indicated that PSNPs are able to enter into the cell nucleus and, in this way, interaction is possible. Although no studies have been carried out with Raji-B cells, we reported confocal studies carried out in Caco-2 cells showing that PSNPs were able to internalize in the cell nucleus, although without apparent genotoxic effects (Cortés et al., 2020).

5. Conclusions

As a summary, in this study, we have demonstrated that exposure of different human hematopoietic cells to PSNPs is able to induce intracellular ROS production and primary DNA damage, as evaluated with the comet assay complemented with FPG enzyme. Nevertheless, these effects are strongly modulated by the cell type. This would indicate that different cell types are needed to have an adequate view of the potential effects of PSNPs. The underlying mechanisms resulting in the higher variability observed between cell-lines would require further studies.

CRediT authorship contribution statement

LR, RM and AH planned the experiments. LR, IB, and JD carried out the experimental part. LR, RM and AH analyzed the data, carried out the statistical analysis, and prepared tables/figures. LR, RM and AH wrote the final manuscript.

Declaration of competing interest

The authors declare that there is no conflict of interest, and are responsible for the content and writing of the article.

Acknowledgments

This investigation was partially supported by the Fondo Nacional de Innovación y Desarrollo Científico y Tecnológico (FONDOCYT) República Dominicana, Proyecto 2018-2019-2B2-093).

L. Rubio held a fellowship from the Spanish Society of Genetics partially supporting her stage at the Universitat Autònoma de Barcelona.

5. References

Andrady, A.L., 2003. Plastic litter and other marine debris. In: Andrady A. L. (ed) Plastics and the environment. Wiley, New York, pp 381–382.

Annangi, B., Bach, J., Vales, G., Rubio, L., Marcos, R., Hernández, A., 2015. Long-term exposures to low doses of cobalt nanoparticles induce cell transformation enhanced by oxidative damage. Nanotoxicology 9, 138-147.

Avio, C.G., Gorbi, S., Milan, M., Benedetti, M., Fattorini, D., d'Errico, G., Pauletto, M., Bargelloni, L., Regoli, F., 2015. Pollutants bioavailability and toxicological risk from microplastics to marine mussels. Environ. Pollut. 198, 211-222.

Barabadi, H., Najafi, M., Samadian, H., Azarnezhad, A., Vahidi, H., Mahjoub, M.A., Koohiyan, M., Ahmadi, A., 2019. A systematic review of the genotoxicity and antigenotoxicity of biologically synthesized metallic nanomaterials: are green nanoparticles safe enough for clinical marketing? Medicina (Kaunas) 55, E439.

Bouwmeester, H., Hollman, P.C.H., Peters, R.J.B., 2015. Potential health impact of environmentally released micro- and nanoplastics in the human food production chain: experiences from nanotoxicology. Environ. Sci. Technol. 49, 8932-8947.

Brandon, J.A., Freibott, A., Sala, L.M., 2020. Patterns of suspended and salp-ingested microplastic debris in the North Pacific investigated with epifluorescence microscopy. Limnol. Ocean. Let. 5, 46-53.

Brandts, I., Teles, M., Gonçalves, A.P., Barreto, A., Franco-Martinez, L., Tvarijonaviciute, A., Martins, M.A., Soares, A.M.V.M., Tort, L., Oliveira, M., 2018. Effects of nanoplastics on *Mytilus galloprovincialis* after individual and combined exposure with carbamazepine. Sci. Total Environ. 643, 775-784.

ChemicaSafetyFacts.org. https://www.chemicalsafetyfacts.org/polystyrene/

Cortés, C., Marcos, R., 2019. The comet assay as a tool to detect the genotoxic potential of nanomaterials. In: A Closer Look at the Comet Assay. K.H. Harmon (Ed.). Nova Science Publ. Inc. New York, Chapter 3, pp 35-64.

Cortés, C., Domenech, J., Salazar, M., Pastor, S., Marcos, R., Hernández, A., 2020. Nanoplastics as a potential environmental health factor: effects of polystyrene nanoparticles on human intestinal epithelial Caco-2 cells. Environ. Sci. Nano 7, 272-285.

Davranche, M., Veclin, C., Pierson-Wickmann, A.C., El Hadri, H., Grassl, B., Rowenczyk, L., Dia, A., Ter Halle, A., Blancho, F., Reynaud, S., Gigault, J., 2019. Are nanoplastics able to bind significant amount of metals? The lead example. Environ. Pollut. 249, 940-948.

Deng, Y., Zhang, Y., Lemos, B., Ren, H., 2017. Tissue accumulation of microplastics in mice and biomarker responses suggest widespread health risks of exposure. Sci. Rep. 7, 46687.

Forte, M., Iachetta, G., Tussellino, M., Carotenuto, R., Prisco, M., De Falco, M., Laforgia, V., Valiante, S., 2016. Polystyrene nanoparticles internalization in human gastric adenocarcinoma cells. Toxicol. In Vitro 31, 126-136.

Fröhlich, E., Meindl, C., Roblegg, E., Ebner, B., Absenger, M., Pieber, T.R., 2012. Action of polystyrene nanoparticles of different sizes on lysosomal function and integrity. Part. Fibre Toxicol. 9, 26.

Gallo, F., Fossi, C., Weber, R., Santillo, D., Sousa, J., Ingram, I., Nadal, A., Romano, D., 2018. Marine litter plastics and microplastics and their toxic chemicals components: the need for urgent preventive measures. Environ. Sci. Eur. 30, 13.

Galloway, S., 2015. Micro- and nano-plastics and human health. In: Bergmann, M., Gutow, L., Klages, M. (eds) Marine Anthropogenic Litter. Springer, Cham International Publishing. Chapter 13, pp 343-366.

Ghezzi, P., 2020. Environmental risk factors and their footprints in vivo - A proposal for the classification of oxidative stress biomarkers. Redox Biol. doi: 10.1016/j.redox.2020.101442. [Epub ahead of print].

Gies, V., Zou, S., 2017. Systematic toxicity investigation of graphene oxide: evaluation of assay selection, cell type, exposure period and flake size. Toxicol. Res. (Camb) 7, 93-101.

Gopinath, P.M., Saranya, V., Vijayakumar, S., Mythili Meera, M., Ruprekha, S., Kunal, R., Pranay, A., Thomas, J., Mukherjee, A., Chandrasekaran, N., 2019. Assessment on interactive prospectives of nanoplastics with plasma proteins and the toxicological impacts of virgin, coronated and environmentally released-nanoplastics. Sci. Rep. 9, 8860.

Hesler, M., Aengenheister, L., Ellinger, B., Drexel, R., Straskraba, S., Jost, C., Wagner, S., Meier, F., von Briesen, H., Büchel, C., Wick, P., Buerki-Thurnherr, T., Kohl, Y., 2019. Multi-endpoint toxicological assessment of polystyrene nano- and microparticles in different biological models in vitro. Toxicol. In Vitro 61, 104610.

Horev-Azaria, L., Baldi, G., Beno, D., Bonacchi, D., Golla-Schindler, U., Kirkpatrick, J.C., Kolle, S., Landsiedel, R., Maimon, O., Marche, P.N., Ponti, J., Romano, R., Rossi, F., Sommer, D., Uboldi, C., Unger, R.E., Villiers, C., Korenstein, R., 2013. Predictive toxicology of cobalt ferrite nanoparticles: comparative in-vitro study of different cellular models using methods of knowledge discovery from data. Part. Fibre Toxicol. 10, 32.

Hussain, N., Jaitley, V., Florence, A.T., 2001. Recent advances in the understanding of uptake of microparticulates across the gastrointestinal lymphatics. Adv. Drug Deliv. Rev. 50, 107-142.

Inkielewicz-Stepniak, I., Tajber, L., Behan, G., Zhang, H., Radomski, M.W., Medina, C., Santos-Martinez, M.J., 2018. The role of mucin in the toxicological impact of polystyrene nanoparticles. Materials 11, 724.

Jani, P., Halbert, G.W., Langridge, J., Florence, A.T., 1990. Nanoparticle uptake by the rat gastrointestinal mucosa: quantitation and particle size dependency. J. Pharm. Pharmacol. 42, 821-826.

Jani, P., Florence, A.T., McCarthy, D.E., 1992. Further histological evidence of the gastrointestinal absorption of polystyrene nanospheres in the rat. Int. J. Pharmac. 84, 245-252.

Lankoff, A., Sandberg, W.J., Wegierek-Ciuk, A., Lisowska, H., Refsnes, M., Sartowska, B., Schwarze, P.E., Meczynska-Wielgosz, S., Wojewodzka, M., Kruszewski, M., 2012. The effect of agglomeration state of silver and titanium dioxide nanoparticles on cellular response of HepG2, A549 and THP-1 cells. Toxicol. Lett. 208, 197-213.

Lehner, R., Weder, C., Petri-Fink, A., Rothen-Rutishauser, B., 2019. Emergence of nanoplastic in the environment and possible impact on human health. Environ. Sci. Technol. 53, 1748-1765.

Lim, S.L., Ng, C.T., Zou, L., Lu, Y., Chen, J., Bay, B.H., Shen, H.M., Ong, C.N., 2019. Targeted metabolomics reveals differential biological effects of nanoplastics and nanoZnO in human lung cells. Nanotoxicology 13, 1117-1132.

Liu, Z., Huang, Y., Jiao, Y., Chen, Q., Wu, D., Yu, P., Li, Y., Cai, M., Zhao, Y., 2020. Polystyrene nanoplastic induces ROS production and affects the MAPK-HIF-1/NFkB-mediated antioxidant system in *Daphnia pulex*. Aquat. Toxicol. 220, 105420.

Loos, C., Syrovets, T., Musyanovych, A., Mailänder, V., Landfester, K., Nienhaus, G.U., Simmet, T., 2014. Functionalized polystyrene nanoparticles as a platform for studying bio-nano interactions. Beilstein J. Nanotechnol. 5, 2403-2412.

Ma, Y., Liu, H., Wu, J., Yuan, L., Wang, Y., Du, X., Wang, R., Marwa, P.W., Petlulu, P., Chen, X., Zhang, H., 2019. The adverse health effects of bisphenol A and related toxicity mechanisms. Environ. Res. 176, 108575.

Magrì, D., Sánchez-Moreno, P., Caputo, G., Gatto, F., Veronesi, M., Bardi, G., Catelani, T., Guarnieri, D., Athanassiou, A., Pompa, P.P., Fragouli, D., 2018. Laser ablation as a versatile tool to mimic polyethylene terephthalate nanoplastic pollutants: characterization and toxicology assessment. ACS Nano 12, 7690-7700.

Mishra, S., Rath, C.C., Das, A.P., 2019. Marine microfiber pollution: a review on present status and future challenges. Mar. Pollut. Bull. 140, 188-197.

Napper, I.E., Bakir, A., Rowland, S.J., Thompson, R.C., 2015. Characterisation, quantity and sorptive properties of microplastics extracted from cosmetics. Mar. Pollut. Bull. 99, 178-185.

Poma, A., Vecchiotti, G., Colafarina, S., Zarivi, O., Aloisi, M., Arrizza, L., Chichiriccò, G., Di Carlo, P., 2019. In vitro genotoxicity of polystyrene nanoparticles on the human fibroblast Hs27 cell line. Nanomaterials (Basel) 9, E1299.

Ribeiro, F., Garcia, A.R., Pereira, B.P., Fonseca, M., Mestre, N.C., Fonseca, T.G., Ilharco, L.M., Bebianno, M.J., 2017. Microplastics effects in *Scrobicularia plana,* Mar. Pollut. Bull. 122, 379-391.

Rubio, L., Marcos, R., Hernández, A., 2019. Potential adverse health effects of ingested micro- and nanoplastics on humans. Lessons learned from in vivo and in vitro mammalian models. J. Toxicol. Environ. Health B Crit. Rev. 23, 53-68.

Schirinzi, G.F., Pérez-Pomeda, I., Sanchís, J., Rossini, C., Farré, M., Barceló, D., 2017. Cytotoxic effects of commonly used nanomaterials and microplastics on cerebral and epithelial human cells. Environ. Res. 159, 579-587.

Sökmen, T.Ö., Sulukan, E., Türkoğlu, M., Baran, A., Özkaraca, M., Ceyhun, S.B., 2019. Polystyrene nanoplastics (20 nm) are able to bioaccumulate and cause oxidative DNA damages in the brain tissue of zebrafish embryo (*Danio rerio*). Neurotoxicology 77, 51-59.

Stock, V., Böhmert, L., Lisicki, E., Block, R., Cara-Carmona, J., Pack, L. K., Selb R., Lichtenstein, D., Voss, L., Henderson, C.J., Zabinsky, E., Sieg, H., Braeuning, A., Lampen, A., 2019. Uptake and effects of orally ingested polystyrene microplastic particles in vitro and in vivo. Arch. Toxicol. 93, 1817-1833.

Tokiwa, Y., Calabia, B.P., Ugwu, C.U., Aiba, S., 2009. Biodegradability of plastics. Int. J. Mol. Sci. 10, 3722-3742.

582 Wright, S.L., Kelly, F.J., 2017. Plastic and human health: a micro issue? Environ. Sci.
583 Technol. 51, 6634-6647.

584 Wright, S.L., Thompson, R.C., Galloway, T.S., 2013. The physical impacts of
585 microplastics on marine organisms: A review. Environ. Pollut. 178, 483-492.

586 Wu, B., Wu, X., Liu, S., Wang, Z., Chen, L., 2019. Size-dependent effects of
587 polystyrene microplastics on cytotoxicity and efflux pump inhibition in human Caco-
588 2 cells. Chemosphere 221, 333-341.

589 Xia, M., Huang, R., Witt, K.L., Southall, N., Fostel, J., Cho, M.H., Jadhav, A., Smith,
590 C.S., Inglese, J., Portier, C.J., Tice, R.R., Austin, C.P., 2008. Compound
591 cytotoxicity profiling using quantitative high-throughput screening. Environ. Health
592 Perspect. 116, 284-291

593 Yu, F., Yang, C., Zhu, Z., Bai, X., Ma, J., 2019. Adsorption behavior of organic
594 pollutants and metals on micro/nanoplastics in the aquatic environment. Sci. Total
595 Environ. 694, 133643.

596

Tables

Table 1. Characterization of PSNPs and fPSNPs dispersions (100 µg/mL), in distilled H_2O and RPMI (10% FBS) culture media, by using the Zetasizer Nano ZS.

	PSNPs		fPSNPs	
Dispersant	Distilled H_2O	RPMI	Distilled H_2O	RPMI
Size (nm) (DLS)	86.33 ± 10.20	142.8 ± 5.68	112.87 ± 3.11	222.4 ± 2.433
PdI (DLS)	0.10 ± 0.09	0.478 ± 0.058	0.35 ± 0.02	0.494 ± 0.036
Z-potential (mV) (DLV)	-36.00 ± 7.88	-11.6 ± 0.850	-45.97 ± 3.84	-10.6 ± 0.529
Mobility (µm cm/Vs) (DLV)	-2.29 ± 0.10	-0.7379 ± 0.0534	-3.76 ± 0.38	-0.6733 ± 0.033

603 **Figure legends**

604

605 **Figure 1.** Size and morphology of both PSNPs and fPSNPs as determined by TEM.
606 TEM images of 100 µg/mL of PSNPs and fPSNPs dispersions in distilled H_2O
607 produced average sizes of 52.99 ± 14.68 nm and 44.19 ± 28.54 nm, respectively.

608

609 **Figure 2.** Relative cell viability of Raji-B, TK6 and THP-1 cells after the exposure to
610 PSNPs at concentrations ranging from 0 to 200 µg/mL, at 24 h (A) and 48 h (B)
611 exposure times. Data are represented as the percentage of living cells relative to the
612 untreated control ± SEM. One-way ANOVA with Dunnett's post-test was used for the
613 statistical analysis. Statistical significance was indicated in the graph as follows, $*P <$
614 0.05, $**P < 0.01$ for Raji-B cell line and $^{\#}P < 0.05$, $^{\#\#}P < 0.01$ for TK6 cell line.

615

616 **Figure 3.** fPSNPs cellular internalization by Raji-B, TK6 and THP-1 cells after
617 exposures lasting for 24 h (A) and 48 h (B). The graph represents the percentage of
618 fluorescent-positive cells over the total cell population. Graphs show the mean ± SEM
619 of three different experiments performed in duplicates. Data are analyzed by the one-
620 way ANOVA test with a Dunnett's post-test.

621

622 **Figure 4.** Relative ROS production in Raji-B, TK6 and THP-1 cells treated with 0 - 50
623 µg/mL of PSNPs for 3 h (A) and 24 h (B) detected using the DCFH-DA assay. Data are
624 represented as mean ± SEM and analyzed by the one-way ANOVA with Dunnett's
625 post-test. Statistical significance was indicated in the graph as follows, $*P < 0.05$ for
626 Raji-B cell line, and $^{\#}P < 0.05$, $^{\#\#}P < 0.01$ for TK6 cell line.

627

628

629 **Figure 5.** Genotoxic damage observed in Raji-B cells by using the comet assay after 3
630 h (A), 24 h (B) and 48 h (C) of PSNPs exposures. The concentration of 200 µM MMS
631 was used as a positive control. Oxidative DNA damage (ODD) was detected using the
632 FPG enzyme. Data are represented as mean ± SEM and analyzed by the one-way
633 ANOVA test with a Dunnett post-test. Statistical significance was indicated in the graph
634 as follows, $*P < 0.05$, $***P < 0.001$ for genotoxic damage and $^{\#\#}P < 0.01$; $^{\#\#\#}P < 0.001$
635 for ODD.

636

637 **Figure 6.** Genotoxic damage observed in TK6 cells by using the comet assay after
638 exposures to PSNPs lasting for 3 h (A), 24 h (B) and 48 h (C). The concentration of
639 200 µM MMS was used as a positive control. Oxidative DNA damage (ODD) was

640 detected using the FPG enzyme. Data are represented as mean ± SEM and analyzed
641 by the one-way ANOVA test with a Dunnett post-test. Statistical significance was
642 indicated in the graph as follows, ***$P < 0.001$ for genotoxic damage and $^{\#}P < 0.05$, $^{\#\#}P$
643 < 0.01; $^{\#\#\#}P < 0.001$ for ODD.
644
645 **Figure 7.** Genotoxic damage observed in THP-1 cells as detected by the comet assay
646 after exposures to PSNPs lasting for 3 h (A), 24 h (B) and 48 h (C). The concentration
647 of 200 µM MMS was used as a positive control. Oxidative DNA damage (ODD) was
648 detected using the FPG enzyme. Data are represented as mean ± SEM and analyzed
649 by the one-way ANOVA with a Dunnett post-test. Statistical significance was indicated
650 in the graph as follows, ***$P < 0.001$ for genotoxic damage and $^{\#\#\#}P < 0.001$ for ODD.

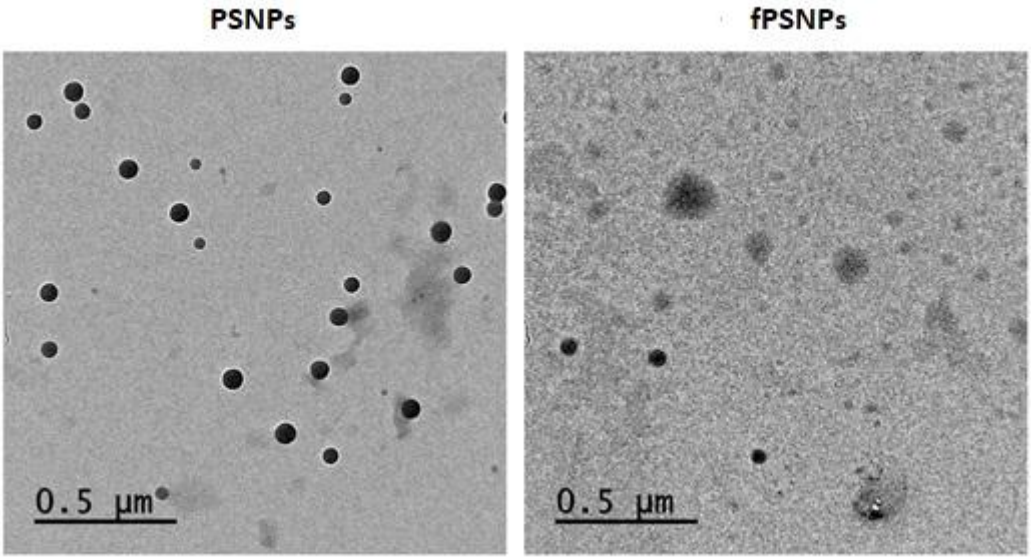

651

652

653 **Figure 1.**

654

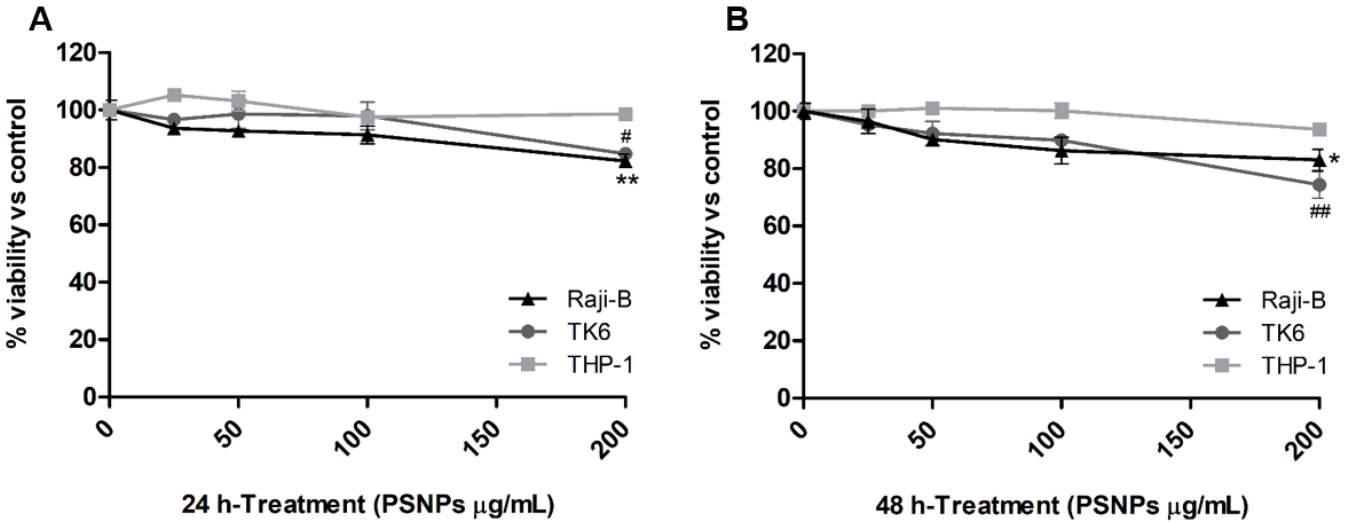

656

657 **Figure 2.**

658

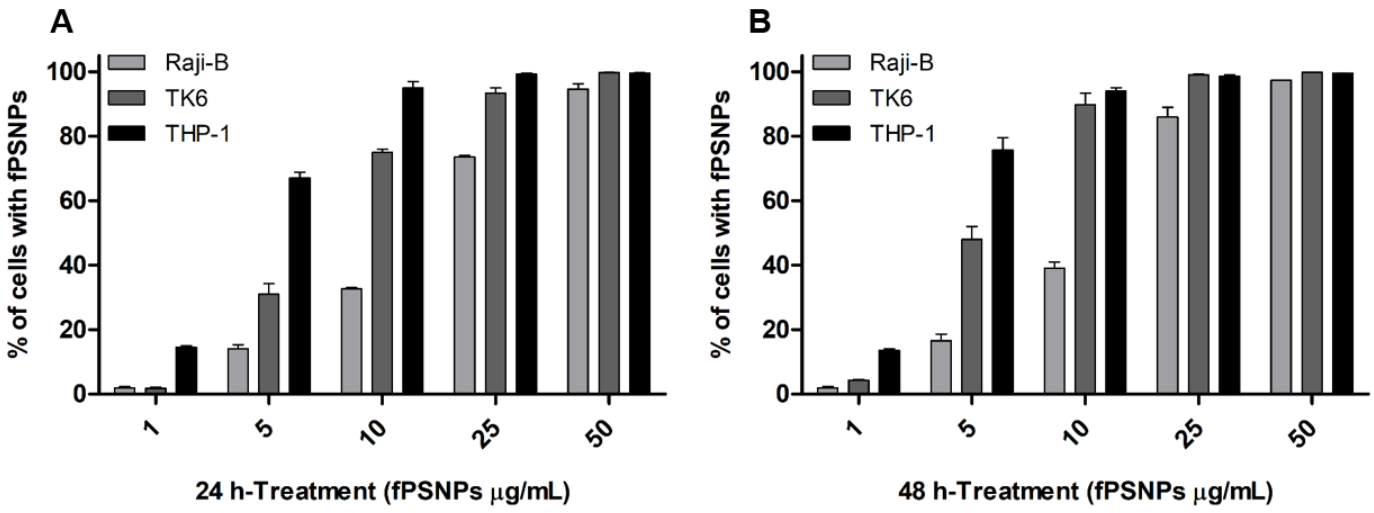

660

661 **Figure 3.**

662

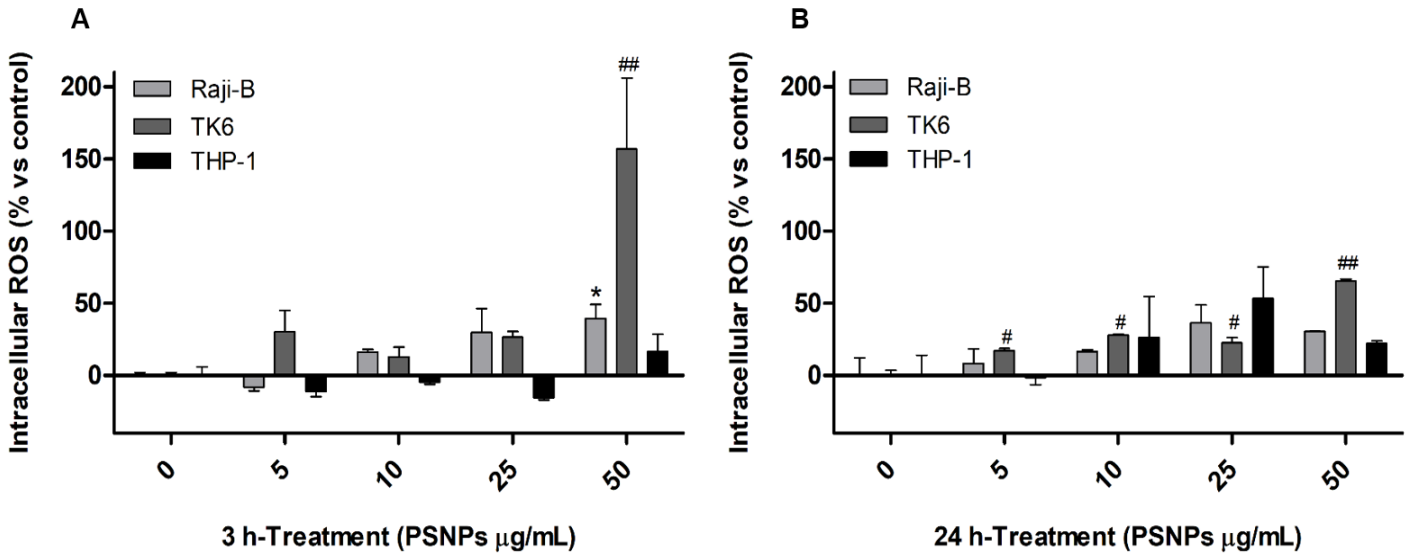

664 **Figure 4.**

665

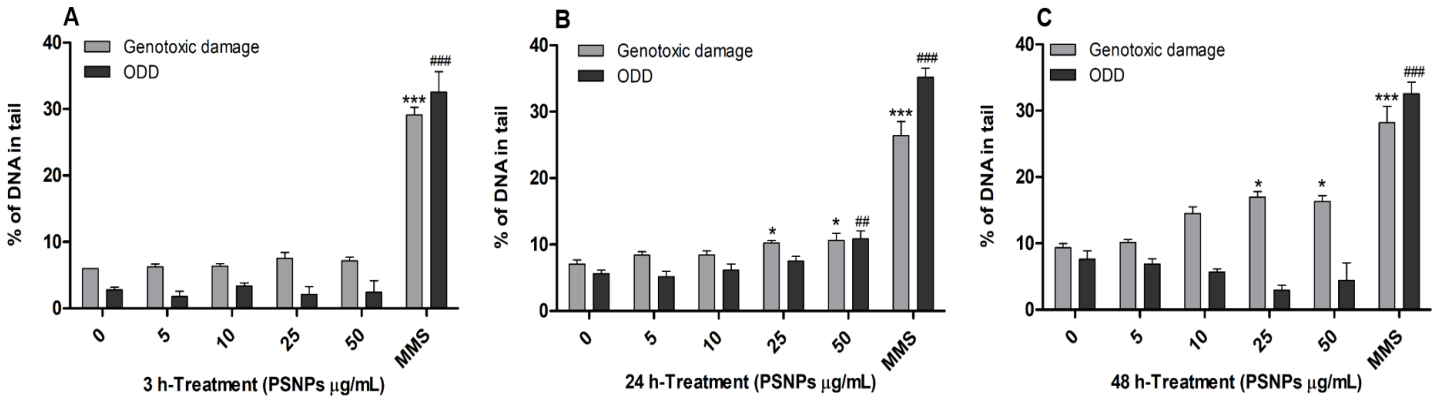

667

668 **Figure 5.**

669

670

671

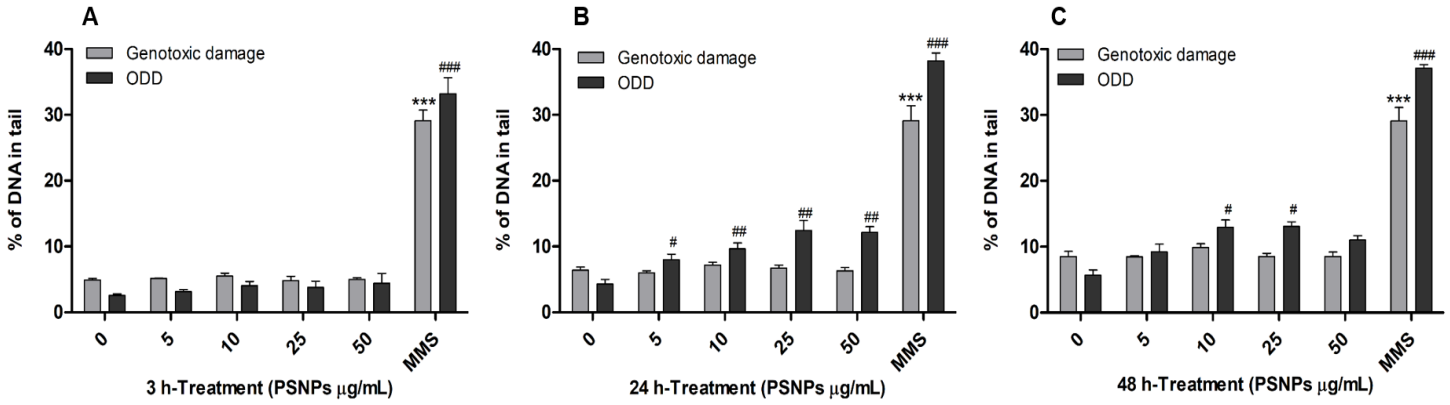

673

674 **Figure 6.**

675

676

677

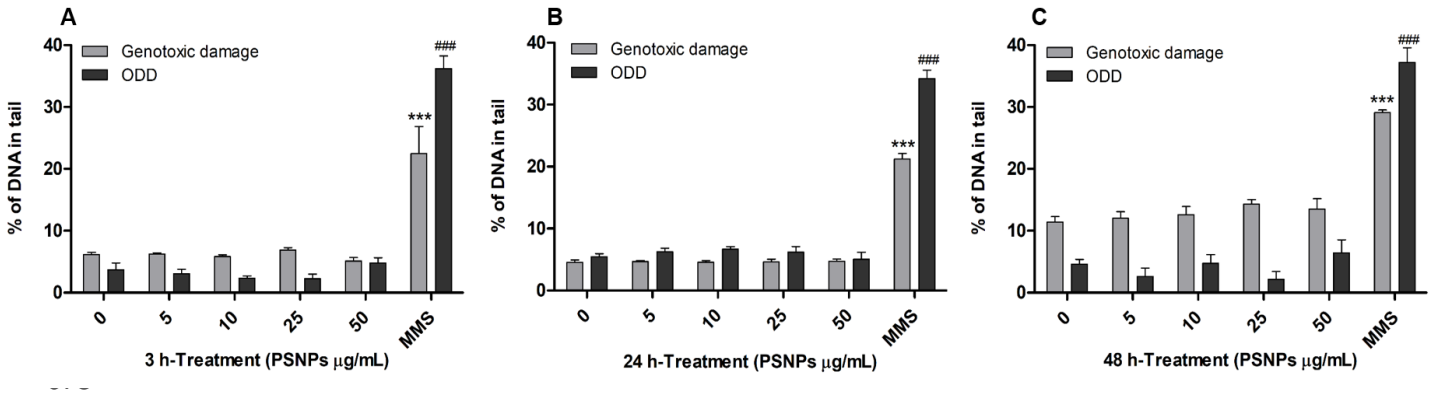

679

680

681 **Figure 7.**

682

683